EMBO reports

scientific report

Trypanosoma cruzi macrophage infectivity potentiator has a rotamase core and a highly exposed α-helix

Pedro José Barbosa Pereira, M. Cristina Vega, Elena González-Rey[1], Rafael Fernández-Carazo[1], Sandra Macedo-Ribeiro[+], F. Xavier Gomis-Rüth, Antonio González[1] & Miquel Coll[‡]

Institut de Biología Molecular-CSIC, Jordi Girona 18-26, E-08034 Barcelona and [1]Instituto de Parasitología y Biomedicina-CSIC, Ventanilla 11, E-18001 Granada, Spain

Received September 4, 2001; revised November 5, 2001; accepted November 16, 2001

The macrophage infectivity potentiator protein from *Trypanosoma cruzi* (TcMIP) is a major virulence factor secreted by the etiological agent of Chagas' disease. It is functionally involved in host cell invasion. We have determined the three-dimensional crystal structure of TcMIP at 1.7 Å resolution. The monomeric protein displays a peptidyl-prolyl *cis–trans* isomerase (PPIase) core, encompassing the characteristic rotamase hydrophobic active site, thus explaining the strong inhibition of TcMIP by the immunosuppressant FK506 and related drugs. In TcMIP, the twisted β-sheet of the core is extended by an extra β-strand, preceded by a long, exposed N-terminal α-helix, which might be a target recognition element. An invasion assay shows that the MIP protein from *Legionella pneumophila* (LpMIP), which has an equivalent N-terminal α-helix, can substitute for TcMIP. An additional exposed α-helix, this one unique to TcMIP, is located in the C-terminus of the protein. The high-resolution structure reported here opens the possibility for the design of new inhibitory drugs that might be useful for the clinical treatment of American trypanosomiasis.

INTRODUCTION

Chagas' disease or American trypanosomiasis is a severe sickness that afflicts 16–18 million people in Central and South America. According to the World Health Organization, it is endemic in 21 countries, where ~100 million people are at risk. Chagas' disease is caused by the flagellated protozoan *Trypanosoma cruzi*, a parasite able to evade the host immune system. The lack of a vaccine and the fact that existing drugs are only partially effective make American trypanosomiasis an essentially incurable disease.

Trypomastigotes are the non-dividing infective forms of the parasite, which penetrate a wide range of phagocytic and non-phagocytic mammalian cells. Invasion of the host cell involves the activation of signal transduction pathways through a series of complex steps, which are not fully understood (Burleigh and Andrews, 1998).

Trypanosoma cruzi macrophage infectivity potentiator (TcMIP) is a peptidyl-prolyl *cis–trans* isomerase (PPIase) secreted by *T. cruzi* trypomastigotes (Moro *et al.*, 1995). MIP proteins have also been reported as virulence factors in the pathogenic intracellular bacteria *Legionella pneumophila* (Engleberg *et al.*, 1989) and *Chlamydia trachomatis* (Lundemose *et al.*, 1991), the etiological agents of human Legionnaires' disease and chlamydiasis, respectively. These PPIases are inhibited by the immunosuppressant macrolide antibiotic FK506, and are thus related to the FK506 binding proteins (FKBPs). In *Saccharomyces cerevisiae*, these proteins mediate the action of FK506 and rapamycin, although they do not appear to be essential for viability (Heitman *et al.*, 1991; Dolinski *et al.*, 1997). Although the enzymatic activity of PPIases is associated with the acceleration of protein folding (Schiene and Fischer, 2000; Schiene-Fischer and Yu, 2001), the mechanism of action of MIPs during host cell invasion remains to be elucidated. In particular, the biological target for the rotamase activity of MIPs has not been identified.

[+]Present address: Faculdade de Ciências e Tecnologia, Universidade do Algarve, 8000 Faro, Portugal
[‡]Corresponding author. Tel: +34 93 4006100; Fax: +34 93 2045904; E-mail: mcccri@cid.csic.es

Here we report the three-dimensional crystal structure of the MIP protein from *T. cruzi* at 1.7 Å resolution. This resolution allows a detailed view of the molecule and, in particular, of the active site, opening the possibility of designing new specific inhibitors that might impair trypanosomal invasion.

RESULTS AND DISCUSSION

Overall structure and active site

TcMIP is a 167-residue monomeric protein with a molecular mass of 18.8 kDa and overall dimensions 57 × 40 × 25 Å^3. It consists of a central catalytic rotamase-like core surrounded by additional helical secondary structure elements (Figure 1A). The core is composed of a six-stranded anti-parallel β-sheet and a short α-helix (α2) (Figure 1B). The β-sheet has 1–2–5–6–3–4 topology and wraps, with a right-handed twist, around helix α2. Strand β4 is split into two segments (termed β4a and β4b), separated by a large seven-residue bulge that includes an α-helical turn. This arrangement resembles a closed left hand, with the fingers represented by the β-strands, wrapping around the thumb, mimicked by helix α2.

Following the left-hand analogy, a long α-helix (α1) is located on top of the fingers, and exposed to the exterior. α-Helix α1 precedes the outermost strand β1, covering most of loop β5–β6 and part of β-strands β1, β2 and β5 (Figure 1B). The N-terminus of helix α1 protrudes from the protein core, with which its C-terminal half makes exclusively hydrophobic contacts, over an area of ~600 Å^2. The second largest helix of TcMIP (α3) is located at the C-terminus of the protein and, unlike helix α1, it has a net negative charge at its surface. Helix α3 is stabilized by salt bridges between Arg72 (of strand β2) and Glu190, and between Arg131 (of loop α2–β6) and Asp183, in addition to hydrophobic contacts with the core of the protein. Because this helix is located at the face of the protein core opposite to the active site, loop β6–α3 crosses over loop β2–β3, with which it forms three main-chain to main-chain hydrogen bonds (Figure 1B).

The active site of TcMIP is located in the palm of the hand and is a deep hydrophobic pocket formed by residues from β-strands β3, β4 and β6, from α-helix α2, and from loop β5–β6 (Figure 2). The side chains of residues Tyr92, Phe102, Asp103, Arg108, Phe114, Val119, Ile120, Tyr146, Ile155 and Phe163 form the walls of this pocket, with the side chain of Trp123 at its bottom. The side chains of residues Tyr92, Asp103 and Arg108 form a hydrogen-bonded cluster.

Comparison with FKBPs and *L. pneumophila* MIP

The central core of TcMIP is structurally similar to that of FKBPs (Michnick *et al.*, 1991; Moore *et al.*, 1991; Van Duyne *et al.*, 1991, 1993; Wilson *et al.*, 1995; Choi *et al.*, 1996; Burkhard *et al.*, 2000; Deivanayagam *et al.*, 2000). FKBPs are functionally similar to other PPIases (e.g. cyclosporins and parvulins), from which they diverge at the primary and tertiary structure levels (Kallen *et al.*, 1991; Wilson *et al.*, 1995; Ranganathan *et al.*, 1997; Deivanayagam *et al.*, 2000). Superposition of TcMIP with human FKBP12 (Van Duyne *et al.*, 1993) reveals 104 topologically equivalent C_α atoms, with a root mean square deviation (r.m.s.d.) of 1.2 Å (Figure 2A). However, in TcMIP the central β-sheet is extended by one extra strand (β1), as described for rabbit FKBP59 (Craescu *et al.*, 1996). The greatest deviations between the rotamase core of TcMIP and FKBP12 occur in loop regions. In TcMIP, loop β4b–α2 is two residues shorter than in human FKBP12, which makes it more compact and allows loop β2–β3 to move in closer, packing between loop β4b–α2 and the segment connecting strand β7 and helix α3. Furthermore, FKBPs lack the surface helices α1 and α3.

The sequence identity of TcMIP with bacterial MIPs ranges from 26 to 38%, with considerable homology in the rotamase core region, while the N- and C-terminal segments differ more (Figure 1A). The first structure of a protein of this family, the macrophage infectivity potentiator protein from *L. pneumophila* (LpMIP), has been reported recently (Riboldi-Tunnicliffe *et al.*, 2001). A structural comparison between TcMIP and LpMIP shows a common fold for the rotamase core (Figure 2A). The two structures have 128 topologically equivalent C_α atoms, with an r.m.s.d. of 1.0 Å. As with TcMIP, the central β-sheet of LpMIP is extended by one extra strand (β1). In addition, loops β4b–α2 and β2–β3 of LpMIP closely resemble those from TcMIP, rather than those of FKBP12.

The structure of the binding pocket of TcMIP is very similar to that of human FKBP12, except for Phe114, whose side chain occupies the position of that of Phe46 in FKBP12 (Figure 2B), replaced in TcMIP by the less bulky Thr112. The void created by the movement of Phe114 is partially filled by the side chain of Leu127, replacing Val63 of FKBP12. The distinct rotamer observed for Phe114 in TcMIP, when compared with FKBP12, is also observed in the active site of LpMIP due to the presence of an alanine residue in the position occupied by Thr112 in TcMIP. The active sites of TcMIP and LpMIP also differ in the H-bonded cluster formed by Tyr92, Asp103 and Arg108, conserved in FKBP12 (Van Duyne *et al.*, 1991, 1993). In LpMIP, Arg108 is replaced by a threonine, thus disrupting the H-bond network.

Helix α1 is longer in LpMIP and is significantly bent along the surface of the protein core, being fixed to the body of the protein by three distinct contacts: a water-mediated H-bond between Asn84 O and Thr199 N, and two main-chain to side chain bonds between Asn84 Nδ2 and Pro196 O, and Ala81 O and Asn197 Nδ2. In TcMIP, Pro160 replaces Thr199 of LpMIP, thus making the first of these contacts impossible. The side chains of Asn84 and Asn197 in LpMIP are replaced in TcMIP by Arg44 and Tyr158, respectively, which no longer form H-bonds with main-chain atoms. At the N-terminus of LpMIP, a not very well defined (with substantially above-average temperature factors) and rather flexible helix bundle domain is involved in the dimerization of the bacterial protein, being absent from the monomeric TcMIP. On the other hand, the C-terminal helix of TcMIP (α3) constitutes a structural element that is unique among MIP-like proteins and rotamases of known structure.

Specific inhibitors

The detailed structural model of TcMIP allows a better understanding of its active-site particularities and raises the possibility of developing novel non-immunosuppressant specific inhibitors of the enzyme. These are valuable research tools for identifying its physiological targets and the infective pathway used by *T. cruzi*; they may also provide novel and promising therapeutic alternatives.

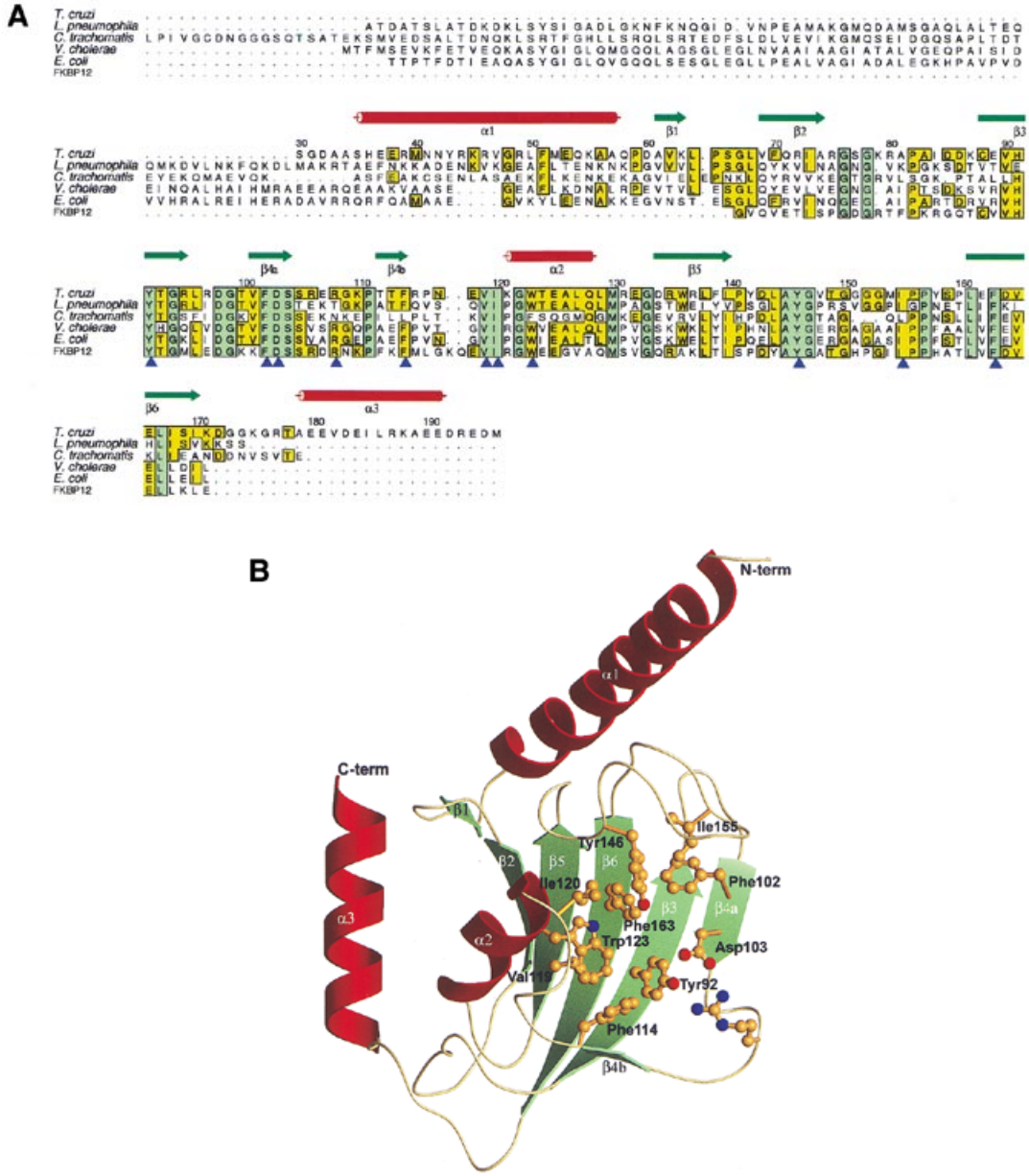

Fig. 1. Structure of TcMIP. (**A**) Amino acid sequence alignment of TcMIP (SWISSPROT entry MIP_TRYCR) with bacterial MIPs from *L. pneumophila* (SWISSPROT entry MIP_LEGPN), *Vibrio cholerae* (SWISSPROT entry Q9KP11) and *C. trachomatis* (SWISSPROT entry MIP_CHLTR), with human FKBP12 (SWISSPROT entry FKB1_HUMAN) and FKBP-like protein from *E. coli* (SWISSPROT entry FKBB_ECOLI). Residues conserved in all sequences are highlighted in green, those identical to TcMIP in yellow. Signal peptide regions have been omitted. Residues forming the hydrophobic active-site pocket are indicated by blue triangles. The numbering and the secondary structure elements of TcMIP are displayed above the alignment. α-Helices are shown in red, β-strands in green. (**B**) Overall structure of TcMIP, with the secondary structure elements shown in red (α-helices) and green (β-strands). The side chains of important residues in the active site of the enzyme are depicted as ball-and-stick models, with carbon atoms in yellow, oxygens in red and nitrogens in blue.

In the absence of a complex of TcMIP with inhibitors, a superposition with FKBP12 in its complexes with the immunosuppressants rapamycin [Protein Data Bank (PDB) code 1c9h; Deivanayagam *et al.*, 2000)] and FK506 (PDB 1bkf; Itoh and Navia, 1995) allows us to analyze the structural determinants of rotamase inhibition (Van Duyne *et al.*, 1993), which can be extrapolated to our model. Both inhibitors are bound in the hydrophobic active-site cavity of FKBP12 between an α-helix and the interior wall of the β-sheet. The common path runs from approximately carbon atom C16 (rapamycin numbering; see Figure 2B) to C31 of the macrolide rings. It includes the deeply penetrating pipecolinyl ring (atoms C2–N7; label A in Figure 2B), attached to the N7–C8 bond, which mimicks the peptide bond proposed to undergo *cis–trans* isomerization in

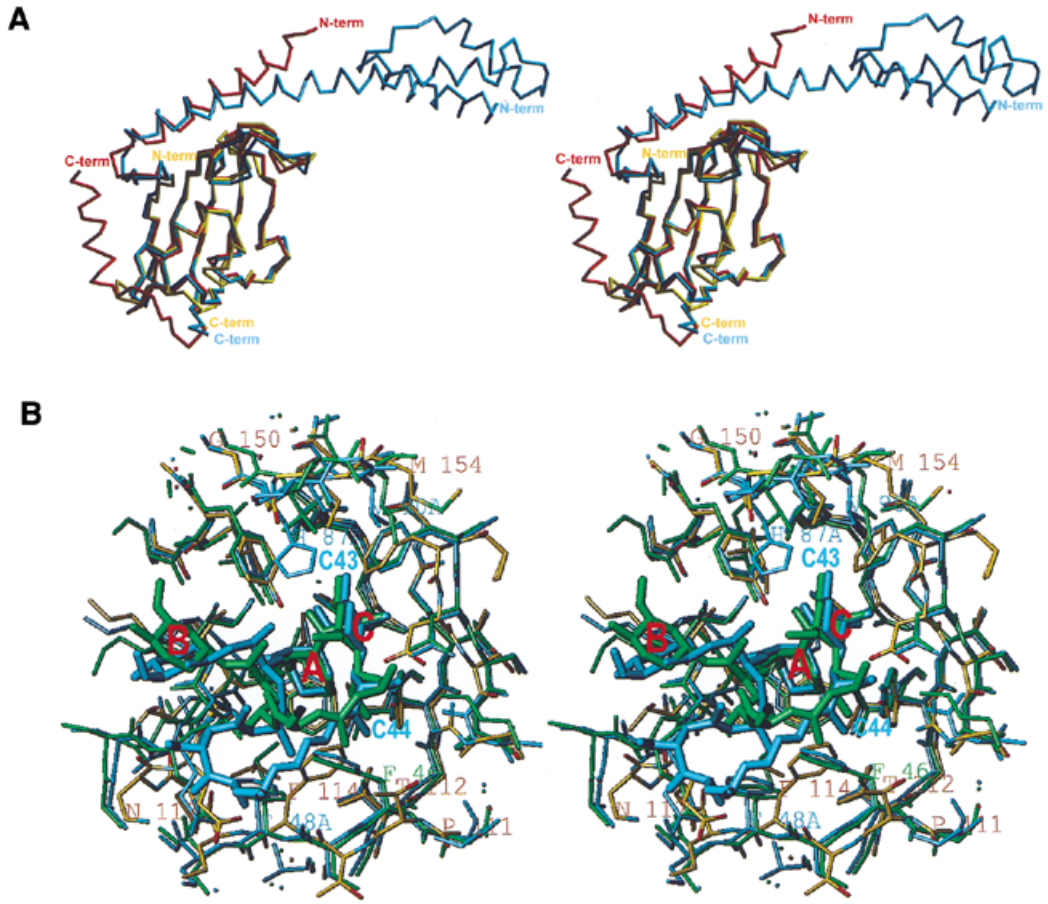

Fig. 2. TcMIP is homologous to other FK506-binding proteins. (**A**) Stereo view of the C_α trace of TcMIP (red) superimposed with those of *L. pneumophila* MIP (blue; PDB code 1FD9) and human FKBP12 (yellow; PDB code 1FKJ). (**B**) Stereo close-up view of the active site of TcMIP (atom colour code) superimposed with that of the human FKBP12–FK506 complex (green; PDB code 1bkf) and the FKBP12–rapamycin complex (blue; PDB code 1c9h). Some key residues and regions of the immunosuppressors discussed in the text are labeled.

a proline-containing substrate in FKBPs and rotamases (Fischer *et al.*, 1993; Orozco *et al.*, 1993), the substituted cyclohexyl moiety attached to main-chain C34 (B in Figure 2B) and the oxacyclohexane group (C10–C14, O5; C in Figure 2B). A detailed inspection of the active-site binding cleft of TcMIP reveals essentially the same features as observed for the immunophilin, in good agreement with the inhibition of TcMIP by FK506 *in vitro*. Protein residues taking part in immunosuppressor binding are equivalent in both enzymes, with the exception of two regions (Figure 2B), which could enable one to design potential drug candidates with a distinct selectivity profile, able to target TcMIP rather than immunophilins. Those regions include the upper rim of the cleft, Gly151-Gly152-Gly153-Met154 of TcMIP (Val/His87-Pro88-Gly89-Ile90 in the FKBP12s studied, see Figure 2B) and the segment forming the cleft base, Thr112-Thr113-Phe114-Arg115-Pro116-Asn117-Glu118 (Phe46-Lys47-Phe48-Met/Arg49-Leu/Ile50-Gly51-Lys52-Gln53-Glu54 in FKBP12s, two residue insertion). Model building indicates that the former could allow for a large hydrophobic group, i.e. a benzyl group, attached to carbon atom C43 (rapamycin numbering), to reside on a hydrophobic pillow made up by the side chains of Tyr146 and Ile155 of TcMIP and, on the other hand, leading to steric clashes in FKBP12 with Val87 and Ile90. The second region affects mainly the anchoring of the pipecolinyl ring A and the attached oxacyclohexane moiety C (Figure 2B). Accordingly, an ethyl group attached to rapamycin C44 would be capable of constructive interactions with TcMIP Thr112 and Phe114, but probably interfere with Phe46 in FKBP.

Hypothetical mechanism of action

Two alternative mechanisms of action can be proposed for TcMIP. In the first, only binding of TcMIP to a protein target—but not its rotamase activity—is necessary to trigger a signal in the host cell, leading to enhanced invasion. The rotamase inhibitor FK506 and its non-immunosuppressant derivative L-685,818, which exhibits antifungal activity (Odom *et al.*, 1997), inhibit TcMIP infectivity (Moro *et al.*, 1995) and block its active site (Figure 2B). Thus, inhibitor binding may hinder the interaction of TcMIP with its physiological target. Alternatively,

the experimentally demonstrated rotamase activity of TcMIP (Moro *et al.*, 1995) could contribute to its action mechanism. The three-dimensional structure of TcMIP reported here shows a FKBP-like core fold, with conserved structure of the active site. Such a stringent three-dimensional conservation is probably driven by maintenance of enzymatic activity.

Pre-treatment of the host with recombinant TcMIP increases *T. cruzi* infectivity, indicating that its target resides in the host cell (Moro *et al.*, 1995). Signaling through transforming growth factor-β receptor (TGFβR) is required for trypanosomal invasion of epithelial cells (Ming *et al.*, 1995), making it a candidate target for TcMIP. However, attempts to induce the expression of a reporter gene under the control of a TGFβ-inducible promoter failed (A. Gonzalez *et al.*, unpublished results), arguing against TGFβR being the natural target of TcMIP.

FKBP12 has been found tightly associated with calcium release channels from both the sarcoplasmic and the endoplasmic reticulum (Collins, 1991; Jayaraman *et al.*, 1992; Cameron *et al.*, 1995). By analogy, TcMIP could bind to transmembrane channels of the host cell, modulating intracellular calcium levels. Mobilization of Ca^{2+} both in the parasite and the target cell during invasion has been reported, while depletion of the intracellular Ca^{2+} concentration hinders invasion (Moreno *et al.*, 1994; Tardieux *et al.*, 1994; Yakubu *et al.*, 1994; Dorta *et al.*, 1995; Rodriguez *et al.*, 1995; Wilkowsky *et al.*, 1996).

A *T. cruzi* infectivity assay was performed in order to compare the effectiveness of TcMIP and LpMIP. As shown in Table I, while 450 nM GST–TcMIP causes a 4-fold increase in the number of internalized parasites (see Methods), a similar concentration of GST–LpMIP causes a 48% increase over controls. Since LpMIP acts as a dimer, its actual concentration in the assay is 225 nM. At 250 nM, TcMIP roughly doubles the number of internalized parasites. These results indicate that LpMIP can effectively substitute for TcMIP and, thus, it is reasonable to believe that, in the assay, they interact in a similar way on a common protein target. In structural terms, both proteins share the conserved rotamase core, and have an additional β-strand in the central β-sheet and an exposed N-terminal α-helix. It is tempting to speculate that helix α1 is a recognition or specificity element in the interaction with the host target protein. The differences in the oligomeric state and between the N-terminal portions of the two proteins could account for the differences observed in their invasion-enhancing action.

Table I. LpMIP can substitute for TcMIP in *T. cruzi* infectivity assay

Added component	No. of internalized parasites/200 cells
Ringer's solution	140 ± 5
450 nM GST	113 ± 8
450 nM GST–LpMIP	192 ± 3
450 nM GST–TcMIP	432 ± 8
250 nM GST–TcMIP	278 ± 13

METHODS

Protein preparation and LpMIP invasion assay. Recombinant TcMIP was produced by scaling up the methods described elsewhere (Moro *et al.*, 1995). After GST removal, TcMIP was further purified by ion-exchange chromatography (MonoQ). The material used for crystallization consists of amino acids 30–196 of TcMIP preceded by an extra glycine residue from the thrombin recognition sequence. The computer-predicted leader peptide cleavage site is located between amino acids 29 and 30.

The coding region of the LpMIP gene, without the leader peptide, was amplified by PCR from *L. pneumophila* strain Philadelphia 1 DNA using specific primers based on the published sequence (Fischer *et al.*, 1992). A fusion protein with GST was expressed in *Escherichia coli* and purified by standard procedures. Cleavage of the fusion protein with thrombin to remove GST resulted in precipitation of LpMIP. Nonetheless, the fusion protein shows rotamase activity levels in good agreement with those published for native LpMIP (Fischer *et al.*, 1992). Furthermore, GST–TcMIP presents slightly higher rotamase activity than TcMIP alone (our unpublished results). An invasion assay was carried out as described previously (Moro *et al.*, 1995) to determine whether GST–LpMIP can functionally replace GST–TcMIP.

Crystallization and data collection. Purified recombinant protein was dialyzed against 5 mM Tris–HCl pH 7.5, 1 mM PMSF and stored at 4°C. Protein crystals of approximate dimensions 0.9 × 0.2 × 0.3 mm^3 appeared spontaneously in this solution within 4–6 weeks. The crystals were harvested in 5 mM Tris–HCl pH 7.5, 10% PEG 6000 and flash frozen in liquid nitrogen prior to data collection. Diffraction data up to 1.7 Å were collected from a single crystal, kept at 100 K, at EMBL beamline BW7B (DESY, Hamburg). The crystals belong to space group $P2_1$ with cell dimensions a = 46.0 Å, b = 34.6 Å, c = 50.4 Å and β = 91.6°, and contain one TcMIP molecule per asymmetric unit (solvent content 41.7%). Data were processed with MOSFLM (Leslie, 1999) and scaled with SCALA (CCP4, 1994). Table II summarizes data collection and processing statistics.

Structure solution and refinement. The structure was solved by molecular replacement with AMoRe (Navaza, 1994), using as a search model the coordinates of residues 88–212 of Lp MIP (PDB code 1FD9), with all non-identical non-glycine residues truncated to alanine. A clear solution was obtained using data in the 15–3.5 Å range, with a correlation coefficient of 19.4 and an R_{factor} of 54.2% (second highest solution: correlation coefficient of 11.4 and an R_{factor} of 56.0%). Cycles of positional and temperature factor refinement with CNS v.1.0 (Brünger *et al.*, 1998), applying bulk solvent and global anisotropic B-factor corrections, alternating with manual model building on a graphic workstation using Turbo-FRODO (Roussel and Cambillau, 1989), allowed us to improve the model and to trace the additional structural elements not included in the rotamase core. Model refinement was completed with SHELX97-2 (Sheldrick and Schneider, 1997), using isotropic thermal parameters. The final model, obtained after a refinement run with all the data, without R_{free} calculation, comprises residues 33–192 of TcMIP (numbering according to the deposited amino acid sequence; SWISSPROT entry MIP_TRYCR) and 271 solvent molecules. All residues are found in allowed regions of the Ramachandran plot, as verified with PROCHECK within (CCP4, 1994), which confirms the high quality of the final model. The three N-terminal residues as well as the C-terminal four amino acids of mature TcMIP are not well defined

Table II. Data collection and processing

Space group	$P2_1$
Cell constants[a]	46.0, 34.6, 50.5, 91.6
Wavelength (Å)	0.885
No. of measurements	60 547
No. of unique reflections	17 009
Whole resolution range (Å)	19.2–1.70
completeness (%)	95.9
R_{merge} (%)[b]	8.1
Last resolution shell (Å)	1.79–1.70
completeness (%)	89.8
R_{merge} (%)[b]	9.7
B-factor (Wilson) (Å^2)	15.6
Average multiplicity	3.6

[a]Values for *a*, *b* and *c* in Å, and β in degrees.
[b]$R_{merge} = [\Sigma_{hkl}\Sigma_i\ |I_i(hkl) - <I(hkl)>| / \Sigma_{hkl}\Sigma_i\ I_i(hkl)] \times 100$, where I_i is the *i*-th measurement of reflection hkl and $<I(hkl)>$ its mean value.

Table III. Refinement statistics

Resolution range (Å)	19.0–1.7
Reflections used for refinement (total/test set)	16 999/863
R_{factor}[a] (%)	17.9
R_{free}[b] (%)	23.1
R.m.s.d. bond lengths	0.005
R.m.s.d. bond angles	1.572
R.m.s.d. bonded *B*-factors	3.3
Average *B*-factor for protein atoms (Å^2)	16.3
Average *B*-factor for solvent atoms (Å^2)	31.2
Non-hydrogen protein atoms	1287
Solvent molecules	271

[a]$R_{factor} = \Sigma_{hkl}\ ||F_{obs}| - k\ |F_{calc}|| / \Sigma_{hkl}\ |F_{obs}|$.
[b]$R_{free} = R_{factor}$ for 5% of reflections not used in refinement.

in the electron density maps and were not included in the present model. Table III presents a summary of the refinement statistics.

Miscellaneous. Structural homology searches were performed with the DALI server (http://www.ebi.ac.uk/dali/). Figure 1A was produced with ALSCRIPT (Barton, 1993), and Figures 1B, 2A and B with SETOR (Evans, 1990). The coordinates have been deposited with the PDB (accession code 1JVW).

ACKNOWLEDGEMENTS

We thank Isabel García-Sáez for help during crystallization and Maria Solà during data collection. This work was supported by grants from Ministerio de Educación y Cultura (PB98-1631 and 2FD97-0518), CSIC and Generalitat de Catalunya (CERBA and 1999SGR188) to M.C., grant PB98-0479 to A.G. and by grant BIO2000-1659 to F.X.G.-R. P.J.B.P. and S.M.-R. acknowledge postdoctoral fellowships from FCT (Portugal). Data collection at DESY was supported by EC grants ERBFMGECT980134 and HPRI-CT-1999-00017 to EMBL-Hamburg.

REFERENCES

Barton, G.J. (1993) ALSCRIPT: a tool to format multiple sequence alignments. *Protein Eng.*, **6**, 37–40.

Brünger, A.T. *et al*. (1998) Crystallography & NMR system: a new software suite for macromolecular structure determination. *Acta Crystallogr. D*, **54**, 905–921.

Burkhard, P., Taylor, P. and Walkinshaw, M.D. (2000) X-ray structures of small ligand–FKBP complexes provide an estimate for hydrophobic interaction energies. *J. Mol. Biol.*, **295**, 953–962.

Burleigh, B.A. and Andrews, N.W. (1998) Signaling and host cell invasion by *Trypanosoma cruzi*. *Curr. Opin. Microbiol.*, **1**, 461–465.

Cameron, A.M., Steiner, J.P., Roskams, A.J., Ali, S.M., Ronnett, G.V. and Snyder, S.H. (1995) Calcineurin associated with the inositol 1,4,5-trisphosphate receptor– FKBP12 complex modulates Ca^{2+} flux. *Cell*, **83**, 463–472.

Choi, J., Chen, J., Schreiber, S.L. and Clardy, J. (1996) Structure of the FKBP12–rapamycin complex interacting with the binding domain of human FRAP. *Science*, **273**, 239–242.

CCP4 (1994) The CCP4 suite: programs for protein crystallography. *Acta Crystallogr. D*, **50**, 760–763.

Collins, J.H. (1991) Sequence analysis of the ryanodine receptor: possible association with a 12K, FK506-binding immunophilin/protein kinase C inhibitor. *Biochem. Biophys. Res. Commun.*, **178**, 1288–1290.

Craescu, C.T., Rouviere, N., Popescu, A., Cerpolini, E., Lebeau, M.C., Baulieu, E.E. and Mispelter, J. (1996) Three-dimensional structure of the immunophilin-like domain of FKBP59 in solution. *Biochemistry*, **35**, 11045–11052.

Deivanayagam, C.C., Carson, M., Thotakura, A., Narayana, S.V. and Chodavarapu, R.S. (2000) Structure of FKBP12.6 in complex with rapamycin. *Acta Crystallogr. D*, **56**, 266–271.

Dolinski, K., Muir, S., Cardenas, M. and Heitman, J. (1997) All cyclophilins and FK506 binding proteins are, individually and collectively, dispensable for viability in *Saccharomyces cerevisiae*. *Proc. Natl Acad. Sci. USA*, **94**, 13093–13098.

Dorta, M.L., Ferreira, A.T., Oshiro, M.E. and Yoshida, N. (1995) Ca^{2+} signal induced by *Trypanosoma cruzi* metacyclic trypomastigote surface molecules implicated in mammalian cell invasion. *Mol. Biochem. Parasitol.*, **73**, 285–289.

Engleberg, N.C., Carter, C., Weber, D.R., Cianciotto, N.P. and Eisenstein, B.I. (1989) DNA sequence of *mip*, a *Legionella pneumophila* gene associated with macrophage infectivity. *Infect. Immunol.*, **57**, 1263–1270.

Evans, S.V. (1990) SETOR: hardware lighted three-dimensional solid model representations of macromolecules. *J. Mol. Graphics*, **11**, 134–138.

Fischer, G., Bang, H., Ludwig, B., Mann, K. and Hacker, J. (1992) Mip protein of *Legionella pneumophila* exhibits peptidyl-prolyl-*cis/trans* isomerase (PPIase) activity. *Mol. Microbiol.*, **6**, 1375–1383.

Fischer, S., Michnick, S. and Karplus, M. (1993) A mechanism for rotamase catalysis by the FK506 binding protein (FKBP). *Biochemistry*, **32**, 13830–13837.

Heitman, J., Movva, N.R. and Hall, M.N. (1991) Targets for cell cycle arrest by the immunosuppressant rapamycin in yeast. *Science*, **253**, 905–909.

Itoh, S. and Navia, M.A. (1995) Structure comparison of native and mutant human recombinant FKBP12 complexes with the immunosuppressant drug FK506 (tacrolimus). *Protein Sci.*, **4**, 2261–2268.

Jayaraman, T., Brillantes, A.M., Timerman, A.P., Fleischer, S., Erdjument-Bromage, H., Tempst, P. and Marks, A.R. (1992) FK506 binding protein

associated with the calcium release channel (ryanodine receptor). *J. Biol. Chem.*, **267**, 9474–9477.

Kallen, J., Spitzfaden, C., Zurini, M.G., Wider, G., Widmer, H., Wüthrich, K. and Walkinshaw, M.D. (1991) Structure of human cyclophilin and its binding site for cyclosporin A determined by X-ray crystallography and NMR spectroscopy. *Nature*, **353**, 276–279.

Leslie, A.G. (1999) Integration of macromolecular diffraction data. *Acta Crystallogr. D*, **55**, 1696–1702.

Lundemose, A.G., Birkelund, S., Fey, S.J., Larsen, P.M. and Christiansen, G. (1991) *Chlamydia trachomatis* contains a protein similar to the *Legionella pneumophila mip* gene product. *Mol. Microbiol.*, **5**, 109–115.

Michnick, S.W., Rosen, M.K., Wandless, T.J., Karplus, M. and Schreiber, S.L. (1991) Solution structure of FKBP, a rotamase enzyme and receptor for FK506 and rapamycin. *Science*, **252**, 836–839.

Ming, M., Ewen, M.E. and Pereira, M.E. (1995) Trypanosome invasion of mammalian cells requires activation of the TGF β signaling pathway. *Cell*, **82**, 287–296.

Moore, J.M., Peattie, D.A., Fitzgibbon, M.J. and Thomson, J.A. (1991) Solution structure of the major binding protein for the immunosuppressant FK506. *Nature*, **351**, 248–250.

Moreno, S.N., Silva, J., Vercesi, A.E. and Docampo, R. (1994) Cytosolic-free calcium elevation in *Trypanosoma cruzi* is required for cell invasion. *J. Exp. Med.*, **180**, 1535–1540.

Moro, A., Ruiz-Cabello, F., Fernandez-Cano, A., Stock, R.P. and Gonzalez, A. (1995) Secretion by *Trypanosoma cruzi* of a peptidyl-prolyl *cis–trans* isomerase involved in cell infection. *EMBO J.*, **14**, 2483–2409.

Navaza, J. (1994) An automated package for molecular replacement. *Acta Crystallogr. A*, **50**, 157–163.

Odom, A., Del Poeta, M., Perfect, J. and Heitman, J. (1997) The immunosuppressant FK506 and its nonimmunosuppressive analog L-685,818 are toxic to *Cryptococcus neoformans* by inhibition of a common target protein. *Antimicrob. Agents Chemother.*, **41**, 156–161.

Orozco, M., Tirado-Rives, J. and Jorgensen, W.L. (1993) Mechanism for the rotamase activity of FK506 binding protein from molecular dynamics simulations. *Biochemistry*, **32**, 12864–12874.

Ranganathan, R., Lu, K.P., Hunter, T. and Noel, J.P. (1997) Structural and functional analysis of the mitotic rotamase Pin1 suggests substrate recognition is phosphorylation dependent. *Cell*, **89**, 875–886.

Riboldi-Tunnicliffe, A., König, B., Jessen, S., Weiss, M.S., Rahfeld, J., Hacker, J., Fischer, G. and Hilgenfeld, R. (2001) Crystal structure of Mip, a prolylisomerase from *Legionella pneumophila*. *Nature Struct. Biol.*, **8**, 779–783.

Rodriguez, A., Rioult, M.G., Ora, A. and Andrews, N.W. (1995) A trypanosome-soluble factor induces IP3 formation, intracellular Ca^{2+} mobilization and microfilament rearrangement in host cells. *J. Cell Biol.*, **129**, 1263–1273.

Roussel, A. and Cambillau, C. (1989) *TurboFRODO in Sillicon Graphics Geometry*. Sillicon Graphics, Mountain View, CA.

Schiene, C. and Fischer, G. (2000) Enzymes that catalyse the restructuring of proteins. *Curr. Opin. Struct. Biol.*, **10**, 40–45.

Schiene-Fischer, C. and Yu, C. (2001) Receptor accessory folding helper enzymes: the functional role of peptidyl prolyl *cis/trans* isomerases. *FEBS Lett.*, **495**, 1–6.

Sheldrick, G.M. and Schneider, T.R. (1997) SHELXL: high resolution refinement. *Methods Enzymol.*, **277**, 319–343.

Tardieux, I., Nathanson, M.H. and Andrews, N.W. (1994) Role in host cell invasion of *Trypanosoma cruzi*-induced cytosolic-free Ca^{2+} transients. *J. Exp. Med.*, **179**, 1017–1022.

Van Duyne, G.D., Standaert, R.F., Karplus, P.A., Schreiber, S.L. and Clardy, J. (1991) Atomic structure of FKBP–FK506, an immunophilin–immunosuppressant complex. *Science*, **252**, 839–842.

Van Duyne, G.D., Standaert, R.F., Karplus, P.A., Schreiber, S.L. and Clardy, J. (1993) Atomic structures of the human immunophilin FKBP-12 complexes with FK506 and rapamycin. *J. Mol. Biol.*, **229**, 105–124.

Wilkowsky, S.E., Wainszelbaum, M.J. and Isola, E.L. (1996) *Trypanosoma cruzi*: participation of intracellular Ca^{2+} during metacyclic trypomastigote–macrophage interaction. *Biochem. Biophys. Res. Commun.*, **222**, 386–389.

Wilson, K.P. *et al.* (1995) Comparative X-ray structures of the major binding protein for the immunosuppressant FK506 (tacrolimus) in unliganded form and in complex with FK506 and rapamycin. *Acta Crystallogr. D*, **51**, 511–521.

Yakubu, M.A., Majumder, S. and Kierszenbaum, F. (1994) Changes in *Trypanosoma cruzi* infectivity by treatments that affect calcium ion levels. *Mol. Biochem. Parasitol.*, **66**, 119–125.

DOI: 10.1093/embo-reports/kvf009